Young Neutron Stars and Their Environments
IAU Symposium, Vol. 218, 2004
F. Camilo and B. M. Gaensler, eds.

Orthogonal Mode Polarization of Pulsar Radio Emission

Q. Luo & D. B. Melrose

School of Physics, The University of Sydney, NSW 2006, Australia

Abstract. We discuss a model for polarization of pulsar radio emission, based on the assumption that waves propagate in two elliptically polarized natural modes. Some results from numerical simulation of single pulses are discussed with emphasis on circular polarization, microstructures and single pulse statistics.

1. Introduction

The rotating vector model (RVM) is successful in explaining observed position angle (PA) variation. Despite the success of the RVM for some pulsars, the usual RVM gives no direct predication of circular polarization (CP). The RVM predicts a smooth PA variation, while a spread in PA and switch between two orthogonal modes (OMs) are often observed.

We consider a model for polarization of pulsar radio emission, based on the conventional RVM but with two OM polarization ellipses derived from the local plasma dispersion with a nonzero charge imbalance $\eta \neq 0$. The radio emission is simulated numerically by assuming a random distribution of many subsources within a confined radial range with emission beamed in a narrow cone.

2. Numerical Modeling of Single Pulses

Single pulses are modeled as superposition of emission from a random distribution of 100% polarized point sources that are not phase connected and can be in either mode. Averaging over the random phases, the Stokes parameters can be obtained as a sum of emission from individual subsources.

The two OM polarization ellipses strongly depend on the plasma parameters such as the propagation angle θ. As the waves propagate away from the source these ellipses vary in both their orientation and ellipticity as the direction of $\mathbf{B}$ and the local plasma parameters change. The polarization of the radiation follows that of the natural modes up to a polarization limiting radius (PLR) beyond which the plasma can no longer significantly change the polarization.

In the cold plasma approximation, the handedness of the ellipses can change when the waves propagate across the critical angle $\theta \sim 1/\Gamma_s$ to the magnetic field line (where Γ_s is the bulk Lorentz factor of the emitting plasma), or cross the local cyclotron frequency Ω_e which varies along the ray path. A self-consistent derivation of the conditions for change of handedness requires inclusion of a relativistic distribution (Melrose & Luo 2004).

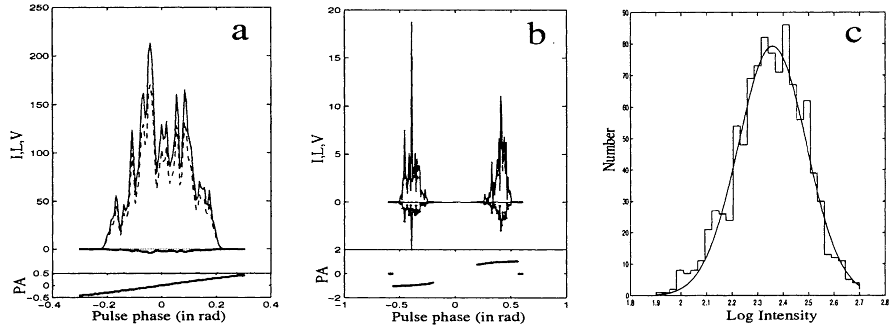

Figure 1. Simulated single pulses (a, b) and intensity distribution (c).

3. Results

Simulated single pulses are shown in Figure 1 for a pulsar with inclination angle $\alpha = \pi/6$ and period $P = 0.1$ s. Figure 1a is obtained with $\Gamma_s = 200$, the viewing angle (relative to the rotation axis) $i = \pi/4 + 0.6$, and the emission location $R_E = 30R_0 - 30.2R_0$ (where R_0 is the star's radius). In Figure 1b we assume $\Gamma_s = 800$, $i = \pi/6 + 0.1$ and $R_E = 20R_0 - 22R_0$. In both cases, one assumes that $\eta = 0.1$, $\Omega_e/\omega_p = 10^4$ and $\omega/\omega_p = 5$, where ω_p is the plasma frequency and ω is the wave frequency (the values apply in the plasma rest frame). The finite beam width of subsources leads to depolarization and scattering in PA. The smaller the decoupling distance (Δs) the broader the scattering in PA. The broad spread in PA observed for some pulsars (e.g., PSRs B0329+54 and B1133+16) can be interpreted as the combination of small Δs and a wider beam width.

A relatively large CP can be obtained for a moderately large propagation angle ($\theta\Gamma_s > 1$). A large CP in the small propagation angle regime ($\theta\Gamma_s \ll 1$) requires emission to be in a very narrow cone. The CP in these two regimes has opposite handedness. Single pulses in Figures 1a and 1b have one sign of CP; this is because only the first regime and only one mode are considered.

The simulated pulses show substructures that are similar to the microstructures seen in observations, with a typical time scale of $\tau_\mu \approx P/2\pi\Gamma_s$. Substructures on a much shorter time scale, $\tau_\mu = R_c/\Gamma_s^3 c$, can be produced by a distribution of subsources along the field line coupled with the effect of the field line curvature (where R_c is the radius of curvature). A still much shorter time scale is possible if subsources radiate with a finite life time $< R_c/\Gamma_s c$.

Single pulse statistics for pulse phase 0.1 rad are shown in Figure 1c as a histogram of probability against log intensity (in relative scale). The solid curve is a lognormal fit. The lognormal fit is in good agreement with observations (e.g., Cairns, Johnston & Das 2001; Kramer, Johnston & van Straten 2002).

References

Cairns, I. H., Johnston, S., & Das, P. 2001, ApJ, 563, L65

Kramer, M., Johnston, S., & van Straten, W. 2002, MNRAS, 334, 523

Melrose, D. B., & Luo, Q. 2004, MNRAS, submitted